Planewave Expansion Methods for Photonic Crystal Fibres

R. A. Norton[a,*], R. Scheichl[b]

[a]*Department of Mathematics and Statistics, La Trobe University, Bundoora, Victoria 3086, Australia,*
Phone: +61 3 9479 2600, Fax:+61 3 9479 2466.
[b]*Department of Mathematical Sciences, University of Bath, BA2 7AY, United Kingdom*

Abstract

Photonic crystal fibres are novel optical devices that can be designed to guide light of a particular frequency. This requires two phenomena to occur. First, the frequency of light must be in a gap of the spectrum of the fibre's cladding (usually a periodic arrangement of air holes), so that the cladding acts as a barrier to that frequency of light. Second, the perturbation or defect in the middle of the fibre must allow a localised or *trapped* mode to exist in a spectral gap of the cladding so that light may propagate inside the defect. In this paper the performance of planewave expansion methods for computing such spectral gaps and trapped eigenmodes in photonic crystal fibres is carefully analysed. The occurrence of discontinuous coefficients in the governing equation means that exponential convergence is impossible due to the limited regularity of the eigenfunctions. However, we show through a numerical convergence study and rigorous analysis on a simplified problem that the planewave expansion method is at least as good as standard finite element schemes on uniform meshes in both error convergence and computational efficiency. More importantly, we also consider the performance of two commonly used variants of the planewave expansion method: (a) coupling the planewave expansion method with a regularisation technique where the discontinuous coefficients in the governing equation are approximated by smooth functions, and (b) approximating the Fourier coefficients of the discontinuous coefficients in the governing equation. There is no evidence that regularisation improves the planewave expansion method, but with the correct choice of parameters both variants can be used efficiently without adding significant errors.

Keywords: planewave expansion method, spectral approximation, Fourier methods, error analysis, smoothing, sampling
2008 MSC: 65N25, 65N12, 65Z05, 65T40

1. Introduction

Photonic crystal fibres (PCFs) are a novel generation of optical fibre and physicists are actively trying to discover and exploit their unique properties. The cross-section of a fibre typically has a periodic structure with a central defect or compact perturbation. Since they are difficult and expensive to manufacture the task of mathematically modelling the behaviour of light in them is very important. In this paper we consider the problem of computing spectral band gaps (that arise from the periodicity) and guided modes (that occur due to the compact perturbation) in PCFs

---

*Corresponding author
Email addresses:* `Richard.Norton@latrobe.edu.au` (R. A. Norton), `R.Scheichl@bath.ac.uk` (R. Scheichl)

using the planewave expansion method. This method is a popular choice for this type of problem, [7, 6, 17, 16, 18].

The propagation of light is governed by Maxwell's equations. A common approach to solve Maxwell's equations in PCFs is to look only for time-harmonic solutions and to exploit symmetries, in particular translational invariance, to simplify the equations to spectral problems with Schrödinger-type operators.

To compute spectral band gaps only the unperturbed periodic structure in the cladding of the fibre needs to be considered. By applying the Floquet-Bloch tranform a family of modified problems on a bounded domain are obtained, with periodic boundary conditions, essential for planewave expansion. The spectrum of the original problem is then obtained by taking the union of the spectra of the family of transformed problems (c.f. [9]). To compute a trapped mode via planewave expansion is more difficult. First, the perturbed coefficient needs to be extended periodically to a larger period cell (the so-called *supercell method*), then the Floquet-Bloch transform can be applied again as above. The trapped mode appears as a narrow band in the essential spectrum of the supercell problem.

Especially in solid state physics, planewave expansion for Schrödinger-type operators is extremely powerful and popular because of its exponential convergence. However, this relies heavily on the smoothness of the potential in those applications and on the resulting high regularity of the eigenfunctions. In the PCF case, the potential and other coefficient functions are not smooth. They are discontinuous at the interface of materials (e.g. between glass and air), which in turn reduces the convergence rate of the planewave expansion method.

In this paper we analyse the convergence of planewave expansion methods for PCF problems. This is achieved through a numerical convergence study and rigorous analysis on a simplified model problem, the Schrödinger operator. We show that the error of the planewave expansion method is comparable to that of standard finite element schemes on uniform meshes, and that it depends entirely on the regularity of the eigenfunctions. Moreover, we show that the planewave expansion method can be implemented with the same computational efficiency as the standard finite element method, by using iterative eigensolvers and a simple and optimal preconditioner. Furthermore, we also consider two variants: (a) coupling the planewave expansion method with a regularisation technique where the discontinuous coefficients are approximated by smooth coefficients (see [11, 7, 16]), and (b) approximating the Fourier coefficients of the discontinuous coefficients in the governing equation via a sampling technique (see e.g. [7, 17, 16, 18, 15]). Variant (b) is usually necessary in practice, because explicit formulae for the Fourier coefficients of the discontinuous coefficients are only available for simple geometries.

A mathematical analysis of the convergence properties of the planewave expansion method for a simplified version of the problem can be found in [14] (including the case of regularisation, but without sampling). Beyond this recent paper there has been relatively little analysis for problems with discontinuous coefficients despite the popularity of the method. There is no analysis of the planewave expansion method with sampling in the literature. Other papers that have analysed various aspects of the planewave expansion method include [21] and [4]. A mathematical paper that performs an analysis for a simplified 1D problem is [12]. Further details of the results presented here can be found in [14] and [13].

The rest of this paper is organised as follows. In §2 we formulate the problem by applying symmetries and the Floquet-Bloch transform. In §3 we give a brief description of the planewave expansion method and how it is implemented, as well as describing the variants: (a) the planewave

expansion method with regularisation, and (b) the planewave expansion method with sampling. Section 4 contains a detailed numerical study of the convergence of these planewave expansion methods. Section 5 is devoted to the mathematical analysis of the planewave expansion method for the Schrödinger operator with (the practically essential) sampling. For completeness we include a short review of results from [14] for the planewave expansion error and regularisation error. Numerical results for sampling are also included here to confirm our theoretical results. Finally, in §6 we make some concluding remarks.

2. Modelling the flow of light in PCFs

We will study source free, non-magnetic PCFs. To describe the structure of a PCF we define its refractive index n on $\mathbb{R}^3$. In this paper we only consider the case when n is piecewise constant. Furthermore, we choose the z-axis parallel to the fibre so that the (x, y)-plane is a cross-section. In this way a PCF is invariant with respect to z and $n = n(x, y)$, and its cross-section can be described as a photonic crystal with a compact perturbation, i.e. $n = n_p + n_c$ where n_p is periodic on some Bravais lattice and n_c is a compact perturbation. Note that instead of applying boundary conditions we define n for all of $\mathbb{R}^3$.

For spectral band gap calculations we only need to perform calculations on the photonic crystal with $n = n_p$, since the addition of a compact perturbation does not change the essential spectrum of the operator (see e.g. [9]). We can define the period cell $\Omega \subset \mathbb{R}^2$ to be the Wigner-Seitz primitive cell of the underlying Bravais lattice (for definitions, see [1]).

To compute a trapped mode, on the other hand, we must include the perturbation. Since $n = n_p + n_c$ is not periodic and the planewave expansion method requires periodicity, we resort to the so-called *supercell method* and replace $n = n_p + n_c$ with $n = n_p^{super}$. We choose a new Bravais lattice with sufficiently large Wigner-Seitz primitive cell $\Omega \subset \mathbb{R}^2$ (the *supercell*) such that $n_p^{super} = n_p + n_c$ in Ω and n_p^{super} is periodic on the new Bravais lattice (i.e. the perturbation is repeated periodically in n_p^{super}).

The accuracy of the supercell approximation has been studied for a simplified problem in [20], but for the more general problem that we consider here a rigorous analysis is still lacking. In [20] it is shown that (for their simplified problem) the error in the essential spectrum of the perturbed periodic problem decays quadratically with the inverse of the distance between perturbations in n_p^{super}, while the error for isolated eigenvalues decays exponentially. See [13, p. 28] for a plot that confirms these convergence rates for the 1D version of the Schrödinger operator that we consider later. Further discussion can be found in [9] and the references therein.

Now that we have defined a piecewise constant, periodic function $n = n(x, y)$ with period cell $\Omega \subset \mathbb{R}^2$, we can exploit symmetries to simplify Maxwell's equations and obtain a Schrödinger–type spectral problem. Eliminating the electric field from time-harmonic Maxwell's equations we obtain

$$\nabla \times (\tfrac{1}{n^2} \nabla \times \mathbf{H}) = k^2 \mathbf{H}, \tag{1}$$

$$\nabla \cdot \mathbf{H} = 0, \tag{2}$$

on $\mathbb{R}^3$ where $\mathbf{H}$ is the magnetic field, k is the wave number and n is the refractive index as defined above. In this paper we consider the problem of finding $\mathbf{H}$ given k and n. Note that this corresponds to fixing the frequency of light. The invariance of n in the z-direction is exploited to simplify (1) and (2) by expanding $\mathbf{H}$ in the form

$$\mathbf{H}(x, y, z) = \mathbf{h}(x, y)\mathrm{e}^{i\beta z} = (\mathbf{h}_t(x, y) + h_z(x, y)\hat{\mathbf{z}})\mathrm{e}^{i\beta z}, \tag{3}$$

3

for constant β and $\mathbf{h}_t = (h_x, h_y, 0)$.[1] Substituting this into (1) and (2) and using the identity $\nabla(\frac{1}{n^2}) = -\frac{1}{n^2}\nabla(\log n^2)$ we discover (after some vector calculus; details in [13]) that it is sufficient to solve the following eigenproblem on $\mathbb{R}^2$ for eigenfunctions $\mathbf{h}_t(x, y)$ and eigenvalues β^2:

$$(\nabla_t^2 + k^2 n^2)\mathbf{h}_t - (\nabla_t \times \mathbf{h}_t) \times (\nabla_t \log n^2) = \beta^2 \mathbf{h}_t, \tag{4}$$

where $\nabla_t = (\frac{\partial}{\partial x}, \frac{\partial}{\partial y}, 0)$. Note that for $\beta \neq 0$, h_z is uniquely determined by $\mathbf{h}_t$ and β using (2), i.e. $h_z = \frac{i}{\beta}\nabla_t \cdot \mathbf{h}_t$. Also, (4) must be considered in the distributional sense because in the case of PCFs the term $\nabla_t \log n^2$ is not a classical function. It is the gradient of a discontinuous, piecewise constant function.

To transform the problem from one that is posed on $\mathbb{R}^2$ to a family of modified problems on a bounded domain we exploit the periodicity of n and apply the Floquet-Bloch transform (cf. [1], [6], [9]). For each so-called quasi-momentum $\boldsymbol{\xi} \in \mathcal{B} \times \{0\}$ (where $\mathcal{B}$ is the 1st Brillouin zone of the Bravais lattice for n, i.e. the closure of the Wigner-Seitz primitive cell of the reciprocal lattice, see [1]) we may write $\mathbf{h}_t$ as

$$\mathbf{h}_t(x, y) = e^{i\boldsymbol{\xi}\cdot\mathbf{x}}\mathbf{u}_t(x, y),$$

where $\mathbf{u}_t = (u_x, u_y, 0)$ is periodic on the same Bravais lattice as n. Thus, the eigenproblem (4), posed on all of $\mathbb{R}^2$, is transformed into a family of eigenproblems

$$(\nabla_t + i\boldsymbol{\xi})^2\mathbf{u}_t + k^2 n^2\mathbf{u}_t - ((\nabla_t + i\boldsymbol{\xi}) \times \mathbf{u}_t) \times (\nabla_t \log n^2) = \beta^2 \mathbf{u}_t, \quad \text{for all } \boldsymbol{\xi} \in \mathcal{B} \times \{0\}, \tag{5}$$

on the bounded domain $\Omega \subset \mathbb{R}^2$ subject to periodic boundary conditions. Solving this family of eigenproblems is the main focus of this paper.

Some authors (e.g. [9],[20]) make the additional assumption that $\beta = 0$ and solve (4) for the eigenvalue k^2. In this case (4) splits into two scalar equations that are referred to as the TE (transverse electric) and TM (transverse magnetic) mode problems. We do not make this assumption in our paper.

3. Planewave expansion methods

Let us briefly recall the standard (plain vanilla) planewave expansion method and apply it to (5). Note however, that this method is not practical for most applications because it assumes explicit forumlae for the Fourier coefficients of n^2 and $\log n^2$. Instead, it is usually necessary to approximate these Fourier coefficients. This is easily and cheaply achieved via the *sampling method* presented below.

3.1. Planewave expansion method (plain vanilla)

Suppose that n is periodic on a Bravais lattice with primitive lattice vectors $\mathbf{a}_1$ and $\mathbf{a}_2$, i.e. $n(\mathbf{x} + k_1\mathbf{a}_1 + k_2\mathbf{a}_2) = n(\mathbf{x})$ for all $\mathbf{x} \in \mathbb{R}^2$, $k_1, k_2 \in \mathbb{Z}$. Let $\mathbf{b}_1$ and $\mathbf{b}_2$ be primitive lattice vectors for the reciprocal lattice and define

$$\mathbb{G} := \{\mathbf{g} \in \mathbb{R}^2 : \mathbf{g} = k_1\mathbf{b}_1 + k_2\mathbf{b}_2, \mathbf{k} \in \mathbb{Z}^2\}.$$

---

[1]Throughout this paper we use subscript t notation to denote the transverse part of a vector, not the time derivative.

For $G \in \mathbb{N}$ define

$$\mathbb{Z}_G^2 := \{\mathbf{k} \in \mathbb{Z}^2 : |\mathbf{k}| \leq G\},$$
$$\mathbb{G}_G := \{\mathbf{g} \in \mathbb{R}^2 : \mathbf{g} = k_1\mathbf{b}_1 + k_2\mathbf{b}_2, \mathbf{k} \in \mathbb{Z}_G^2\},$$
$$\mathcal{S}_G := \operatorname{span}\{e^{i\mathbf{g}\cdot\mathbf{x}} : \mathbf{g} \in \mathbb{G}_G\}.$$

Let $N := \dim \mathcal{S}_G$. To apply the planewave expansion method to (5) we search for approximations to the eigenfunction $\mathbf{u}_t = (u_1, u_2, 0)$, such that $u_1, u_2 \in \mathcal{S}_G$. For $j = 1, 2$ we may write

$$u_j(\mathbf{x}) = \sum_{\mathbf{g}\in\mathbb{G}_G} [u_j]_\mathbf{g} e^{i\mathbf{g}\cdot\mathbf{x}}, \qquad \mathbf{x} \in \mathbb{R}^2,$$

where $[u_j]_\mathbf{g}$ are the degrees of freedom.[2] Similarly, we expand the coefficient functions in (5) in terms of planewaves, i.e.

$$n^2(\mathbf{x}) = \sum_{\mathbf{k}\in\mathbb{G}} [n^2]_\mathbf{k} e^{i\mathbf{k}\cdot\mathbf{x}} \quad \text{and} \quad \nabla_t \log n^2(\mathbf{x}) = \sum_{\mathbf{k}\in\mathbb{G}} i\mathbf{k}[\log n^2]_\mathbf{k} e^{i\mathbf{k}\cdot\mathbf{x}},$$

and substitute these (together with the expansion of $\mathbf{u}_t$) into (5):

$$\sum_{\mathbf{g}\in\mathbb{G}_G} (i\mathbf{g} + i\boldsymbol{\xi})^2 [\mathbf{u}_t]_\mathbf{g} e^{i\mathbf{g}\cdot\mathbf{x}} + \sum_{\mathbf{g}\in\mathbb{G}_G}\sum_{\mathbf{k}\in\mathbb{G}} k^2 [n^2]_\mathbf{k} [\mathbf{u}_t]_\mathbf{g} e^{i(\mathbf{g}+\mathbf{k})\cdot\mathbf{x}}$$

$$- \sum_{\mathbf{g}\in\mathbb{G}_G}\sum_{\mathbf{k}\in\mathbb{G}} ((i\mathbf{g} + i\boldsymbol{\xi}) \times [\mathbf{u}_t]_\mathbf{g}) \times (i\mathbf{k})[\log n^2]_\mathbf{k} e^{i(\mathbf{g}+\mathbf{k})\cdot\mathbf{x}} = \beta^2 \sum_{\mathbf{g}\in\mathbb{G}_G} [\mathbf{u}_t]_\mathbf{g} e^{i\mathbf{g}\cdot\mathbf{x}},$$

where $[\mathbf{u}_t]_\mathbf{g} = ([u_1]_\mathbf{g}, [u_2]_\mathbf{g}, 0)$. Finally, by comparing coefficients, we obtain the following system of $2N$ equations

$$\sum_{\mathbf{g}\in\mathbb{G}_G} \begin{pmatrix} \mathcal{A}_{11} & \mathcal{A}_{12} \\ \mathcal{A}_{21} & \mathcal{A}_{22} \end{pmatrix} \begin{pmatrix} [u_1]_\mathbf{g} \\ [u_2]_\mathbf{g} \end{pmatrix} = \beta^2 \begin{pmatrix} [u_1]_{\mathbf{g}'} \\ [u_2]_{\mathbf{g}'} \end{pmatrix} \qquad \forall \mathbf{g}' \in \mathbb{G}_G, \tag{6}$$

where the $\mathcal{A}_{ij}$ are given by

$$\mathcal{A}_{11}(\mathbf{g}', \mathbf{g}) = -|\boldsymbol{\xi} + \mathbf{g}|^2 \delta_{\mathbf{g},\mathbf{g}'} + k^2 [n^2]_{\mathbf{g}'-\mathbf{g}} + (g_2' - g_2)(\xi_2 + g_2)[\log n^2]_{\mathbf{g}'-\mathbf{g}},$$
$$\mathcal{A}_{12}(\mathbf{g}', \mathbf{g}) = \qquad\qquad\qquad\qquad\qquad - (g_2' - g_2)(\xi_1 + g_1)[\log n^2]_{\mathbf{g}'-\mathbf{g}},$$
$$\mathcal{A}_{21}(\mathbf{g}', \mathbf{g}) = \qquad\qquad\qquad\qquad\qquad - (g_1' - g_1)(\xi_2 + g_2)[\log n^2]_{\mathbf{g}'-\mathbf{g}},$$
$$\mathcal{A}_{22}(\mathbf{g}', \mathbf{g}) = -|\boldsymbol{\xi} + \mathbf{g}|^2 \delta_{\mathbf{g},\mathbf{g}'} + k^2 [n^2]_{\mathbf{g}'-\mathbf{g}} + (g_1' - g_1)(\xi_1 + g_1)[\log n^2]_{\mathbf{g}'-\mathbf{g}}.$$

This system of equations can be written as a $2N \times 2N$ matrix eigenproblem

$$A\mathbf{v} = \lambda\mathbf{v}, \tag{7}$$

where $\lambda = \beta^2$ is the eigenvalue and the Fourier coefficients $[u_1]_\mathbf{g}$ and $[u_2]_\mathbf{g}$ make up the eigenvector $\mathbf{v}$. In practice we choose an ordering so that A has block form

$$A = \begin{bmatrix} A_{11} & A_{12} \\ A_{21} & A_{22} \end{bmatrix}$$

---

[2] Our convention is to express the index–$\mathbf{g}$ Fourier coefficient in the planewave expansion of a function v by $[v]_\mathbf{g}$.

and each $N \times N$ submatrix A_{ij} has entries that correspond to the coefficients $\mathcal{A}_{ij}$ above. The ordering within each submatrix is in ascending order of magnitude of the moduli of $\mathbf{g}$ and $\mathbf{g}'$, i.e. we define a bijection $i : \mathbb{G}_G \to \{m \in \mathbb{N} : m \leq N\}$ such that $i(\mathbf{g}) < i(\mathbf{g}')$ if $|\mathbf{g}| < |\mathbf{g}'|$. Then $(A_{ij})_{i(\mathbf{g}'),i(\mathbf{g})} = \mathcal{A}_{ij}(\mathbf{g}', \mathbf{g})$ for all $\mathbf{g}, \mathbf{g}' \in \mathbb{G}_G$.

The matrix eigenproblem (7) is solved using a Krylov subspace iteration method, because only a few eigenvalues of A are of physical interest. We use the implicitly restarted Arnoldi method that is implemented in the ARPACK software package [10] applied to $(\sigma I - A)^{-1}$ for a suitably chosen shift σ. At each iteration the action of $(\sigma I - A)^{-1}$ is required, or equivalently, we must solve a linear system with $(\sigma I - A)$. We use preconditioned GMRES [8] with a block preconditioner

$$P = \sigma I - \begin{bmatrix} P_{11} & P_{12} \\ P_{21} & P_{22} \end{bmatrix}$$

with $N \times N$ submatrices P_{ij} chosen to be of the form

$$P_{11} = \begin{bmatrix} B_{11} & 0 \\ 0 & D_{11} \end{bmatrix}, \quad P_{12} = \begin{bmatrix} B_{12} & 0 \\ 0 & 0 \end{bmatrix}, \quad P_{21} = \begin{bmatrix} B_{21} & 0 \\ 0 & 0 \end{bmatrix}, \quad P_{22} = \begin{bmatrix} B_{22} & 0 \\ 0 & D_{22} \end{bmatrix}.$$

In particular, if the blocks B_{ij} are chosen to be the $N_B \times N_B$ principal parts of A_{ij}, for $i, j = 1, 2$ and $1 \leq N_B \leq N$, and the blocks D_{ii} are the diagonals of the remaining $(N - N_B)$ columns and rows of A_{ii}, i.e.

$$(B_{ij})_{k\ell} = (A_{ij})_{k\ell} \qquad \text{for } i, j = 1, 2 \text{ and } k, \ell = 1, \dots, N_B,$$

$$(D_{ii})_{kk} = (A_{ii})_{kk} \qquad \text{for } i = 1, 2 \text{ and } k = 1, \dots, (N - N_B),$$

then the preconditioner P is optimal in practice, in the sense that in all our experiments the number of iterations required by the GMRES method does not depend on the size of N. See [14] for a rigorous proof of the optimality of the preconditioner P in the context of the Schrödinger operator considered later.

Importantly, apart from the application of the preconditioner, the implicitly restarted Arnoldi method with GMRES solver only requires matrix vector products with A, which for the planewave expansion method are available in $\mathcal{O}(G^2 \log G)$ operations using the Fast Fourier Transform (2 FFTs and 4 inverse FFTs). For more details see [13] and [15]. Thus, the total computational cost of solving (7) is $\mathcal{O}(G^2 \log G)$ (or equivalently $\mathcal{O}(N \log N)$).

3.2. Planewave expansion method with regularisation

A method that has been suggested for improving the convergence rate of the planewave expansion method is to replace the discontinuous coefficient function $n(\mathbf{x})$ with an *effective* smooth coefficient function $\widetilde{n}(\mathbf{x})$ (e.g. see [7], [16], [11] and [15]).

Although this can indeed improve the convergence rate of the planewave expansion method (with respect to G or N), the modified method is converging to the solution of the regularised problem and the total error includes an additional error due to regularisation, which needs to also be taken into account. We will quantify the total error below and try to answer the question whether regularisation is beneficial or not.

In this paper we focus on the type of regularisation used in [16] and [15], although we expect similar results to hold for other techniques. Suppose f is a piecewise constant function that is

periodic on a Bravais lattice (e.g. $f = n^2$ or $f = \log n^2$). Then a smooth approximation to f may be given by

$$\widetilde{f}(\mathbf{x}) := (\mathcal{G}_\Delta * f)(\mathbf{x}) = \int_{\mathbb{R}^2} \mathcal{G}_\Delta(\mathbf{x} - \mathbf{y}) f(\mathbf{y}) \mathrm{d}\mathbf{y},$$

where $\mathcal{G}_\Delta$ is the normalised Gaussian,

$$\mathcal{G}_\Delta(\mathbf{x}) := \frac{1}{2\pi\Delta^2} \exp\left(\frac{|\mathbf{x}|^2}{2\Delta^2}\right).$$

The standard deviation of the Gaussian $\Delta > 0$ is the smoothing parameter. As $\Delta \to 0$, $\widetilde{f} \to f$ in the distributional sense. If f is a distribution (e.g. $f = \nabla \log n^2$) then we define $\widetilde{f}$ in a similar way, except we use the distributional notion of convolution. Other types of regularisation might involve taking $\mathcal{G}_\Delta$ to be some other function (e.g. a sinc function).

Gaussian smoothing has the very convenient property that

$$[\widetilde{f}]_\mathbf{g} = [f]_\mathbf{g} \exp\left(-\frac{|\mathbf{g}|^2\Delta^2}{2}\right), \qquad \text{for all} \quad \mathbf{g} \in \mathbb{G}.$$

Using this formula we easily obtain the matrix eigenproblem for the regularised problem by replacing $[n^2]_\mathbf{g}$ and $[\log n^2]_\mathbf{g}$ in the definition of (7) with $[n^2]_\mathbf{g} \exp(-|\mathbf{g}|^2\Delta^2/2)$ and $[\log n^2]_\mathbf{g} \exp(-|\mathbf{g}|^2\Delta^2/2)$, respectively. Thus, the computational cost for planewave expansion with smoothing is the same as that of the plain vanilla version.

3.3. Planewave expansion method with sampling

The planewave expansion method, with and without regularisation, requires knowledge of the Fourier coefficients of n^2 and $\log n^2$. In the definition of (7) we require $[n^2]_\mathbf{g}$ and $[\log n^2]_\mathbf{g}$ for all $\mathbf{g} \in \mathbb{G}_{2G}$. However, except in special cases, explicit formulae are usually not available and it is essential in practice to approximate these Fourier coefficients. This adds an additional error to the calculations. We are interested in the relative size of this additional error and in how the corresponding parameters should be chosen in an optimal way.

A simple and commonly used method to approximate the Fourier coefficients of a periodic function f is to take an FFT of the nodal values of f on a uniform grid in the spatial domain (as opposed to the frequency domain). We call this method *sampling* (see e.g. [7, 17, 16, 18, 15]). The advantage of this method is that all of the Fourier coefficients of f are computed cheaply using a single FFT. This allows us to *oversample* by taking the grid spacing of the corresponding FFT grid significantly finer than that of the FFT grids used in solving (7), without a too large computational penalty.

To define (and analyse) the sampling method it is useful to define, for $M \in \mathbb{N}$,

$$\mathbb{Y}_M^2 := \{\mathbf{k} \in \mathbb{Z}^2 : -\tfrac{M}{2} \le k_i < \tfrac{M}{2}\},$$
$$\mathbb{B}_M := \{\mathbf{x} \in \mathbb{R}^2 : \mathbf{x} = \tfrac{1}{M}(k_1\mathbf{a}_1 + k_2\mathbf{a}_2), \mathbf{k} \in \mathbb{Y}_M^2\},$$
$$\mathbb{H}_M := \{\mathbf{g} \in \mathbb{R}^2 : \mathbf{g} = k_1\mathbf{b}_1 + k_2\mathbf{b}_2, \mathbf{k} \in \mathbb{Y}_M^2\},$$
$$\mathcal{T}_M := \mathrm{span}\{e^{i\mathbf{g}\cdot\mathbf{x}} : \mathbf{g} \in \mathbb{H}_M\}.$$

The set $\mathbb{Y}_M^2$ is a square grid in $\mathbb{R}^2$, $\mathbb{B}_M$ is a uniform grid (not necessarily square) in Ω with grid spacing M^{-1}, $\mathbb{H}_M$ are the corresponding indices for the Fourier coefficients in reciprocal space, and

$\mathcal{T}_M$ is a finite dimensional subspace of planewaves (similar to $\mathcal{S}_G$). We also define (see e.g. [19]), for any $f \in L_p^2 \cap C^0(\mathbb{R}^2)$, the trigonometric projection operator $Q_M : L_p^2 \cap C^0(\mathbb{R}^2) \to \mathcal{T}_M$ by

$$(Q_M f)(\mathbf{x}) := f(\mathbf{x}) \qquad \forall \mathbf{x} \in \mathbb{B}_M. \tag{8}$$

Here, L_p^2 is the space of periodic functions (with respect to the underlying Bravais lattice) that are square integrable on any compact subset of $\mathbb{R}^2$. $C^0(\mathbb{R}^2)$ denotes as usual the space of continuous functions on $\mathbb{R}^2$. If $f \notin C^0(\mathbb{R}^2)$, but only piecewise continuous (e.g. in the case of n^2 and $\log n^2$), then the nodes $\mathbf{x} \in \mathbb{B}_M$ may fall on an interface. Therefore, we extend the definition of Q_M to $Q_M : L_p^2 \to \mathcal{T}_M$ by specifying that

$$Q_M f(\mathbf{x}) := \limsup_{\epsilon \to 0} \frac{1}{|B(\mathbf{x},\epsilon)|} \int_{B(\mathbf{x},\epsilon)} f(\mathbf{y}) \mathrm{d}\mathbf{y} \qquad \forall \mathbf{x} \in \mathbb{B}_M.$$

In the sampling method we approximate n^2 and $\log n^2$ with $Q_M n^2$ and $Q_M \log n^2$, respectively, for a suitably chosen, large M. In practice this means replacing $[n^2]_{\mathbf{g}}$ and $[\log n^2]_{\mathbf{g}}$ in the definition of (7) with $[Q_M n^2]_{\mathbf{g}}$ and $[Q_M \log n^2]_{\mathbf{g}}$, respectively. This is very easy to do in practice and requires only one application of FFT for each function, e.g. computing $\{[Q_M n^2]_{\mathbf{g}} : \mathbf{g} \in \mathbb{H}_M\}$ from $\{(Q_M n^2)(\mathbf{x}) = n^2(\mathbf{x}) : \mathbf{x} \in \mathbb{B}_M\}$ requires only $\mathcal{O}(M^2 \log M)$ operations. Using quadrature to individually approximate each of the Fourier coefficients $[n^2]_{\mathbf{g}}$ and $[\log n^2]_{\mathbf{g}}$ would be much more computationally intensive.

For the overall accuracy of the method it is important to choose M appropriately. It is tempting to use the same size of Fourier grid as in the matrix-vector multiplication with A in the implementation of the iterative eigensolver for (7). However, our analysis and numerical simulations below show that the error contribution from sampling is relatively large and it is better to *oversample* by taking M significantly larger than $2G$. Since only two FFTs (one for n^2 and one for $\log n^2$) with this larger grid are necessary this is no huge penalty in practice, but asymptotically speaking planewave expansion with sampling requires $\mathcal{O}(M^2 \log M + G^2 \log G)$ operations.

4. Numerical Convergence Study

Unfortunately, a theoretical convergence analysis for the full PCF problem (5) is beyond any currently available approaches, and so we have not yet managed to extend our theory for Schrödinger operators in [14] to (5). However, the numerical experiments in this section suggest a very similar behaviour of the planewave expansion method for this much harder problem. The convergence rate is again directly linked to the regularity of the eigenfunctions, although a clear convergence rate is much harder to discern here.

4.1. Setup for numerics

To study the performance of the planewave expansion method for (5) we will use two model examples. They correspond to photonic crystal structures where the background medium is glass ($n = 1.4$) with square air holes ($n = 1$). In Example 1 we are interested in computing spectral gaps for photonic crystals without defect, i.e. $n = n_p$. For this we choose $\Omega = (-\frac{1}{2}, \frac{1}{2})^2$, let n be a simple step function with 3:1 glass to air ratio and $k = 16\pi^2$. This corresponds to light with wavelength $1/2$ (relative to the width of the period cell Ω). $\mathcal{B}$ is $[-\pi, \pi]^2$. Example 2 is reminiscent of the problem of finding a localised mode in a spectral gap of Example 1 where the compact
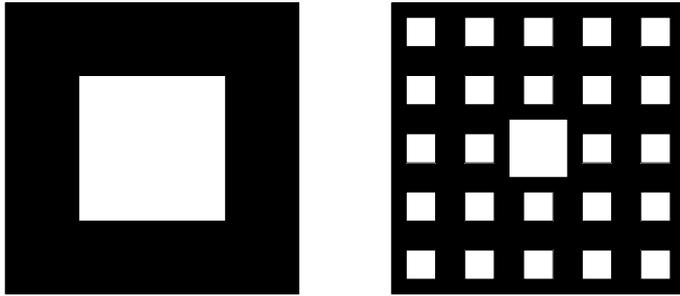
Figure 1: Plot of $n(x, y)$ in Ω for Examples 1 (left) and 2 (right). The scale of n in Example 2 is such that a period cell from Example 1 is the same size as a cell in the cladding of n in Example 2. The black regions are glass ($n = 1.4$) and the white regions correspond to air ($n = 1$).

perturbation consists of one period cell in the periodic structure being replaced by air. We choose a 5×5 supercell so that $\Omega = (-\frac{5}{2}, \frac{5}{2})^2$ and $\mathcal{B} = [-\frac{\pi}{5}, \frac{\pi}{5}]^2$. Therefore, in the supercell problem between each defect there are 4 period cells of the photonic crystal from Example 1. See Figure 1 for a plot of n for these two examples. In our experiments the reference solutions for Examples 1 and 2 were computed with $G = 2^9 - 1$. This corresponds to a matrix eigenproblem (7) of dimension $2N \approx 2 \times 10^6$ (since $N \approx \pi G^2$) and FFTs of size $N_f = (4G + 4) \times (4G + 4) = 2^{11} \times 2^{11}$. Note that for efficiency purposes G is chosen such that the size N_f of the FFT grid is a power of 2.

To measure eigenfunction error, let us define the *gap* between two subspaces X, Y of a Hilbert space $\mathcal{H}$ with norm $\| \cdot \|_{\mathcal{H}}$ to be

$$\delta_{\mathcal{H}}(X, Y) := \sup_{x \in X, \|x\|_{\mathcal{H}} = 1} \mathrm{dist}(x, Y).$$

Here, and throughout this paper, the eigenfunction error is the gap between two subspaces spanned by the corresponding eigenfunctions where $\mathcal{H}$ is H_p^1, the space of periodic functions that lie in the Sobolev space H^1 on any compact subset of $\mathbb{R}^2$. The H_p^1 norm measures the sum of the errors in the function value and its derivative over a period cell.

4.2. Planewave expansion method (plain vanilla)

Figure 2 suggests that the planewave expansion method applied to (5) has an eigenfunction error measured in the H_p^1 norm that is (in general) of $\mathcal{O}(G^{-1/2})$ while the eigenvalue error is $\mathcal{O}(G^{-1})$. This agrees with the theory in [14] about the relationship between regularity of the exact eigenfunctions and convergence rate. Although we do not have a rigorous proof (this is the subject of our current research), we expect (5) to have eigenfunctions with regularity that are one Sobolev–order lower than that of the eigenfunctions of the problem studied in [14] (see also Section 5), leading to a convergence rate for the planewave expansion method that is also one order slower. Consequently, due to the doubling of the convergence rate for the eigenvalue in symmetric eigenproblems, the eigenvalue error is two orders slower. The fact that the eigenvalues of (5) are real and the eigenvalue error decays at twice the rate of the eigenfunction error suggests that (5) is equivalent to a symmetric eigenproblem. This observation may be useful for future theoretical analyses. Moreover, for the eigenfunction error in (5) measured in the L_p^2–norm (5) we would expect to see $\mathcal{O}(G^{-1})$.
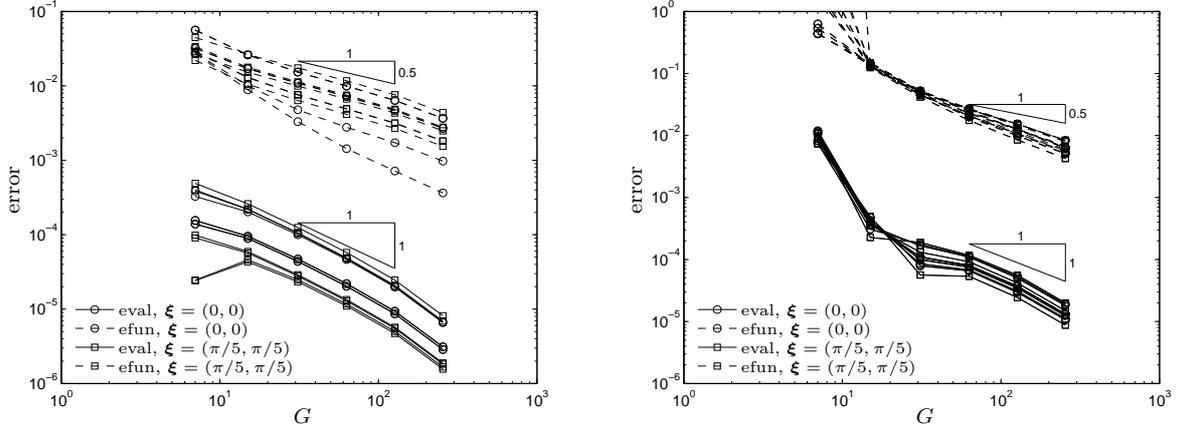
Figure 2: Planewave epansion method (plain vanilla) applied to (5) for Example 1 (left) and Example 2 (right). Plotting the relative eigenvalue error (`eval`) and the eigenfunction error in H_p^1 (`efun`) versus G (first 6 eigenpairs in Ex. 1 with $\boldsymbol{\xi} = (0,0)$ and $\boldsymbol{\xi} = (\pi,\pi)$; 21st-30th eigenpair in Ex. 2 with $\boldsymbol{\xi} = (0,0)$ and $\boldsymbol{\xi} = (\frac{\pi}{5}, \frac{\pi}{5})$).
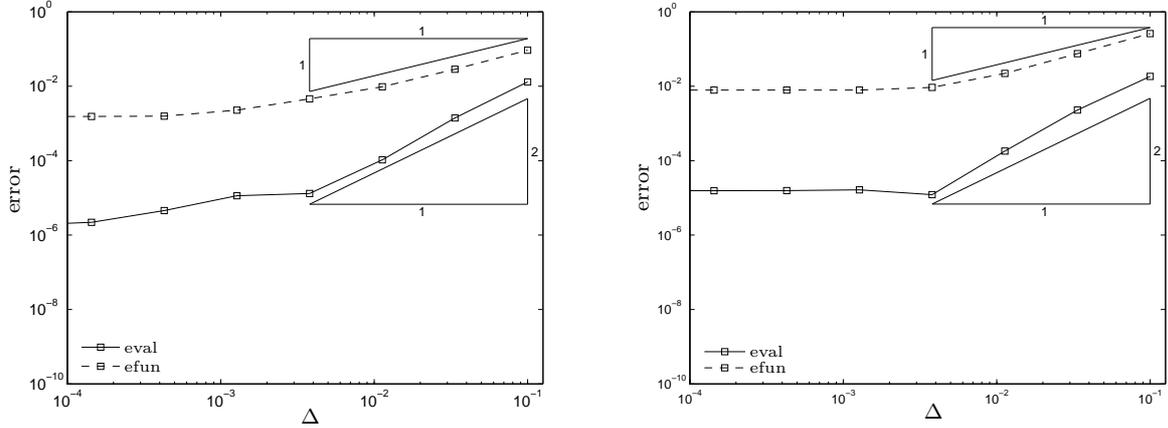

Figure 3: Planewave expansion method with regularisation applied to (5) for Examples 1 (left) and 2 (right). Plotting the relative eigenvalue error (`eval`) and the eigenfunction error in H_p^1 (`efun`) for the 1st eigenpair versus Δ (using $G = 2^8 - 1$, $\boldsymbol{\xi} = (\pi,\pi)$ in Example 1 and $\boldsymbol{\xi} = (\frac{\pi}{5}, \frac{\pi}{5})$ in Example 2).

4.3. Planewave expansion method with regularisation

Let us now consider the regularised planewave expansion method for (5). The error now consists of two contributions, the regularisation error and the approximation error. Figure 3 suggests that for fixed G, while the regularisation error dominates, the eigenfunction error measured in the H_p^1 norm is $\mathcal{O}(\Delta)$ and the eigenvalue error is $\mathcal{O}(\Delta^2)$. For Δ sufficiently small the approximation error dominates and so the overall error does not decrease any longer. To minimise the error and to try and recover (or improve on) the error of the plain vanilla version, we plot in Figure 4 the errors for various choices of $\Delta = G^r$, $r \leq -1/2$, and compare them to $\Delta = 0$ (i.e. plain vanilla, no regularisation). We see that none of the choices for the smoothing parameter Δ beats the un-regularised method for (5). Even though initially, for values of $r < -1/2$, the faster convergence rate of the regularisation error would seem to suggest a faster convergence rate also for the total error in the eigenvalue case, due to the approximation error, asymptotically the total error never converges faster than that of the plain vanilla method. Thus, there is no evidence that regularisation
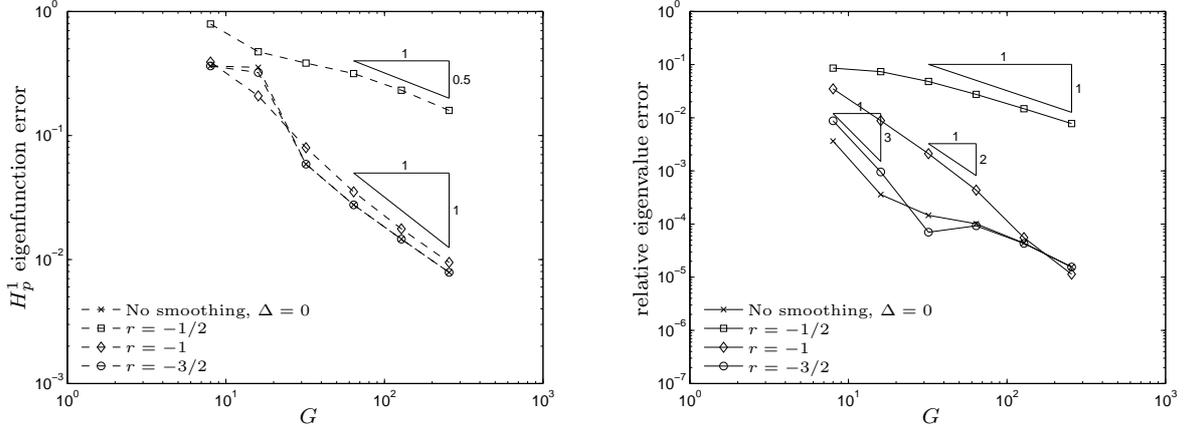
10

Figure 4: Planewave expansion method with regularisation applied to (5) for Example 2. Plotting the error (eigenfunction error in H_p^1 on the left, relative eigenvalue error on the right) for the 1st eigenpair versus G (using $\Delta = 0$ and $\Delta = G^r$ for $r = -\frac{1}{2}, -1, -\frac{3}{2}$ with $\boldsymbol{\xi} = (\frac{\pi}{5}, \frac{\pi}{5})$).
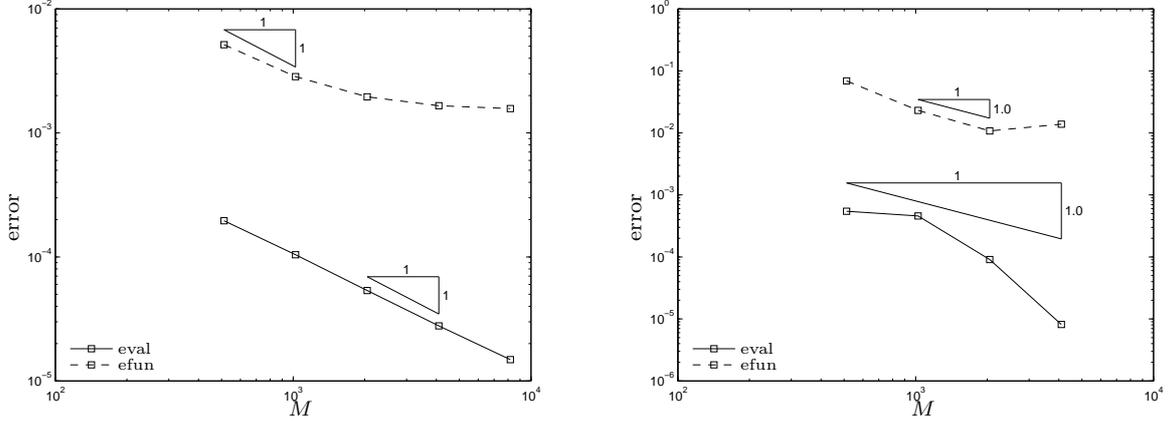

Figure 5: Planewave expansion method with sampling applied to (5) for Examples 1 (left) and 2 (right). Plotting the relative eigenvalue error (`eval`) and the H_p^1 eigenfunction error (`efun`) for the 1st eigenpair versus M (using $G = 2^8 - 1$, $\xi = (\pi, \pi)$ in Example 1 and $\xi = (\frac{\pi}{5}, \frac{\pi}{5})$ in Example 2).

improves the planewave expansion method.

4.4. Planewave expansion method with sampling

In Figure 5, it is hard to discern a clear convergence rate for the errors due to sampling the coefficients in (5). Aliasing effects lead to seemingly faster convergence over some ranges of M while they lead to slower convergence over other ranges (especially in Example 2). Only the eigenvalue error in Example 1 shows a clear convergence rate of $\mathcal{O}(M^{-1})$, but all of the other errors seem to converge roughly with $\mathcal{O}(M^{-1})$. However, the numerical experiments do not conclusively exclude the possibility that the eigenfunction error converges more slowly. The picture for the simplified model problem studied in Section 5 seems clearer. There, both the eigenvalue and eigenfunction error converge with $\mathcal{O}(M^{-1})$ (cf. Figure 8). In Figures 6 and 7 we experiment with choosing $M = \mathcal{O}(G^r)$ for different values of $r \in \mathbb{R}$. To recover an eigenvalue error of $\mathcal{O}(G^{-1})$ observed in the plain vanilla version of planewave expansion, it is clear that we should choose at least $r \geq 1$. Moreover, the results in Figures 6 and 7 show that the eigenvalue errors for exact Fourier coefficients
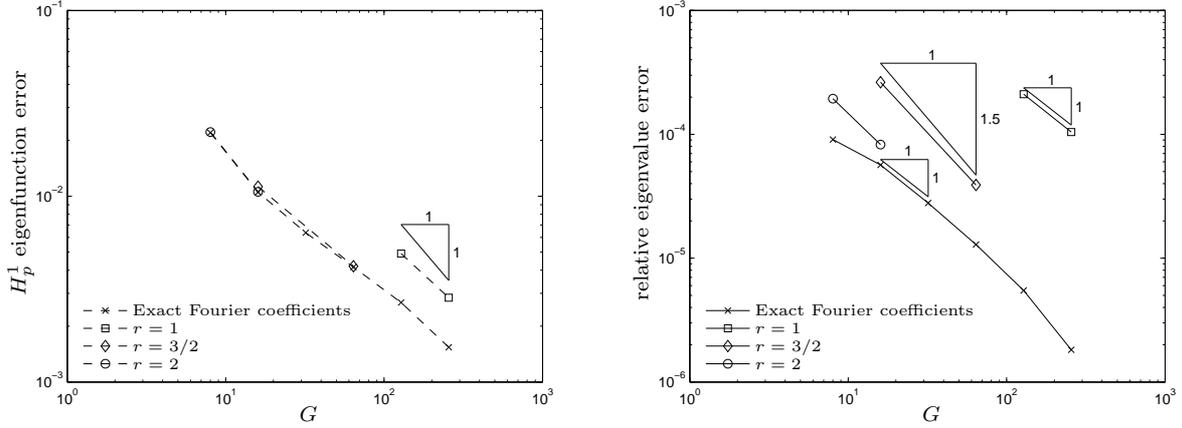
Figure 6: Planewave expansion method with sampling applied to (5) for Example 1. Plotting the error (eigenfunction on the left; eigenvalue on the right) for the 1st eigenpair versus G with exact Fourier coefficients and with $M = \mathcal{O}(G^r)$ for different choices of r ($\boldsymbol{\xi} = (\pi, \pi)$).
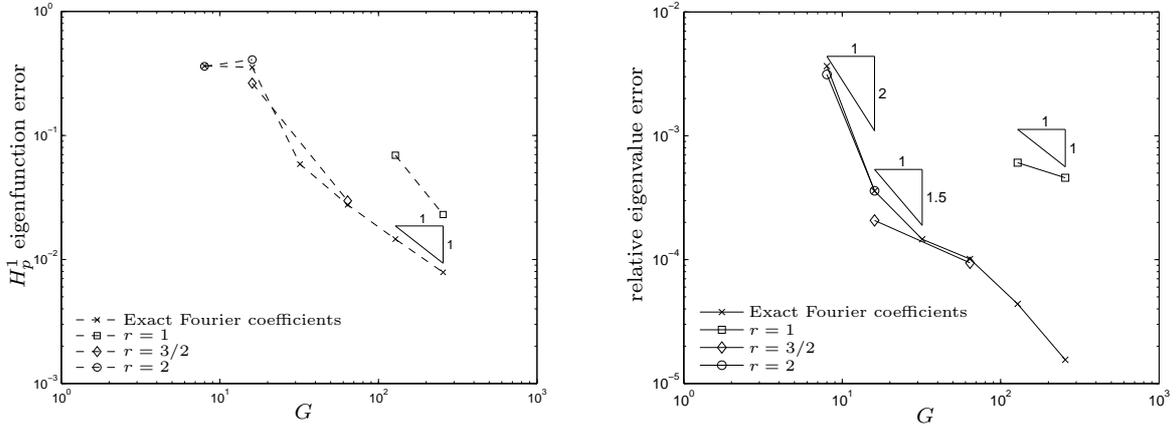

Figure 7: Planewave expansion method with sampling applied to (5) for Example 2. Plotting the error (eigenfunction on the left; eigenvalue on the right) for the 1st eigenpair versus G with exact Fourier coefficients and with $M = \mathcal{O}(G^r)$ for different choices of r ($\boldsymbol{\xi} = (\frac{\pi}{5}, \frac{\pi}{5})$).

can be recovered only with some oversampling, i.e. $r > 1$. For the eigenfunction error a choice of $r = 1$ seems sufficient, confirming that sampling seems to be an efficient method to approximate the Fourier coefficients of n^2 and $\log n^2$ in the case of PCF modelling. The situation is similar when smoothing and sampling are combined and we will address this further for the simplified model problem in the next section.

5. Analysis of a Model Problem

Since we were not able to theoretically analyse the accuracy of planewave expansion methods applied to the full PCF problem, we restrict our attention to the Schrödinger operator in this section. This is necessary because even to determine the regularity of eigenfunctions of (5) is a difficult problem (which is the subject of our current research). The analysis in this section should thus be seen as an important step towards fully understanding planewave expansion methods applied to PCF problems.

12

The simplified problem which we will now consider is

$$(\nabla_t + i\boldsymbol{\xi})^2 u + k^2 n^2 u = \beta^2 u, \qquad \text{for all } \boldsymbol{\xi} \in \mathcal{B} \times \{0\}, \tag{9}$$

on $\Omega \subset \mathbb{R}^2$, again subject to periodic boundary conditions. The only difference to (5) is that the term $((\nabla_t + i\boldsymbol{\xi}) \times \mathbf{h}_t) \times (\nabla_t \log n^2)$ has been dropped. In fact, when the contrast between the maximum and minimum values of n is small, it is physically justified to ignore this term (cf. [3]).

The plain vanilla version of the planewave expansion method described in Section 3 for (5) can be applied in a very similar way to (9). Following the derivation of (6), approximate solutions $\beta^2 \in \mathbb{R}$ and $u \in \mathcal{S}_G$ for (9) can be found by solving the linear system

$$\sum_{\mathbf{g} \in \mathbb{G}_G} \left(-|\mathbf{g} + \boldsymbol{\xi}|^2 \delta_{\mathbf{g}',\mathbf{g}} + k^2 [n^2]_{\mathbf{g}'-\mathbf{g}} \right) [u]_\mathbf{g} = \beta^2 [u]_{\mathbf{g}'} \qquad \forall \mathbf{g}' \in \mathbb{G}_G, \ \forall \boldsymbol{\xi} \in \mathcal{B} \times \{0\}. \tag{10}$$

Regularisation and/or sampling are then applied in the same way as for the full PCF problem (5). More details can be found in [14] and [13].

5.1. Review of existing theory

The plain vanilla planewave expansion method and the planewave expansion method with regularisation for (9) have been analysed in detail in [14], and we now briefly review some of the results. For simplicity we consider only piecewise constant functions n with polygonal interfaces with a finite number of corners that are periodic on square Bravais lattices. It is possible to consider also more general interfaces, but then the details are more complicated (cf. [14]). To extend the results to more general lattices, it suffices to map back to the square lattice first.

Let us define periodic Sobolev spaces. Let H_p^s be the usual periodic Sobolev space with index $s \in \mathbb{R}$ and norm

$$\|u\|_{H_p^s}^2 := \sum_{\mathbf{g} \in \mathbb{G}} |\mathbf{g}|_\star^{2s} |[u]_\mathbf{g}|^2 \qquad \text{where} \qquad |\mathbf{g}|_\star := \begin{cases} 1, & \text{if } \mathbf{g} = 0, \\ |\mathbf{g}|, & \text{if } \mathbf{g} \neq 0. \end{cases}$$

Then $L_p^2 \equiv H_p^0$ and the usual $L^2(\Omega)$-norm is equivalent to the H_p^0-norm. The assumptions we just made on n imply that $n^2 \in H_p^s$ for all $s < 1/2$ (see [14] for details).

For the analysis it is useful to study (9) in shifted weak form, i.e. find $\lambda \in \mathbb{R}$ and $u \in H_p^1$ such that

$$a(u,v) = \lambda b(u,v) \qquad \text{for all } v \in H_p^1, \tag{11}$$

where

$$a(u,v) := \int_\Omega (\nabla_t + i\boldsymbol{\xi})u \cdot \overline{(\nabla_t + i\boldsymbol{\xi})v} + (\sigma - k^2 n^2)u\overline{v}\,\mathrm{d}x\mathrm{d}y \quad \text{and} \quad b(u,v) := \int_\Omega u\overline{v}\,\mathrm{d}x\mathrm{d}y.$$

The shift constant σ is chosen so that $\sigma > k^2 n^2 + 2|\boldsymbol{\xi}|^2$ for all $\mathbf{x} \in \Omega$ and $\boldsymbol{\xi} \in \mathcal{B} \times \{0\}$. This ensures that $a(\cdot,\cdot)$ is coercive in H_p^1 and we identify λ with $\sigma - \beta^2$.

It is a simple exercise to show that (10) is equivalent to a spectral Galerkin method applied to (11), i.e. find $\lambda_G \in \mathbb{R}$ and $u_G \in \mathcal{S}_G$ such that

$$a(u_G, v_G) = \lambda_G b(u_G, v_G) \qquad \text{for all } v_G \in \mathcal{S}_G. \tag{12}$$

The error in solving (12) instead of (11) is the same as the error in applying the planewave expansion method to (9). It is (12) that is analysed in [14]. The main result that was proved in [14] is as follows. It applies standard theory in e.g. [2].

13

Theorem 1. *Let λ be an eigenvalue of* (11) *with multiplicity m and corresponding m-dimensional eigenspace E. Then for G sufficiently large and $\epsilon > 0$ arbitrarily small, there exist m eigenvalues $\lambda_1, \lambda_2, \ldots, \lambda_m$ of* (12) *(counted according to their multiplicity) with corresponding eigenspaces $E_1, \ldots, E_m \subset \mathcal{S}_G$ such that* [3]

$$\delta_{H_p^1}\left(E, \bigoplus_{j=1}^m E_j\right) \lesssim_\epsilon G^{-3/2+\epsilon}, \quad \delta_{L_p^2}\left(E, \bigoplus_{j=1}^m E_j\right) \lesssim_\epsilon G^{-5/2+\epsilon} \quad and \quad |\lambda - \lambda_j| \lesssim_\epsilon G^{-3+\epsilon}$$

for $j = 1, \ldots, m$.

This result shows that the eigenvalue error is almost $\mathcal{O}(G^{-3})$ while the eigenfunction error (measured in the H_p^1–norm) is almost $\mathcal{O}(G^{-3/2})$. This result was clearly supported by numerical experiments in [14] (cf. [14, Fig. 2]). The key step in the proof of the above theorem was to show that the operator $T : L_p^2 \to H_p^1$, defined for any $f \in L_p^2$ by

$$a(Tf, v) = b(f, v), \qquad \text{for all} \ \ v \in H_p^1, \tag{13}$$

is a smoothing operator with

$$\|Tf\|_{H_p^{5/2-\epsilon}} \lesssim_\epsilon \|f\|_{H_p^1} \qquad \text{for any } \epsilon > 0. \tag{14}$$

Using the fact that (λ, u) is an eigenpair of (11) if and only if (λ^{-1}, u) is an eigenpair of T, it is a simple corollary of (14) that all eigenfunctions of (11) are in $H_p^{5/2-\epsilon}$ for all $\epsilon > 0$. The proof merely exploits this regularity to obtain the convergence rates for the eigenfunctions in H_p^1. A functional analysis trick (see e.g. [2]) doubles this convergence rate for the eigenvalues, and a simple duality argument leads to the L_p^2 bound.

Remark 2. In (5) the discontinuous coefficient appears in a higher derivative term than in (9). We expect this to reduce the regularity of the eigenfunctions of (5) to $H_p^{3/2-\epsilon}$, thus also reducing the convergence rate in the eigenfunctions for the planewave expansion method by one order. Even though we have been unable (so far) to extend our analysis to the (un-simplified) PCF problem (5), we have observed this reduced convergence rate in our numerical experiments in Section 4.2.

The following theorem, taken again from [14], bounds the total error due to planewave expansion *and* regularisation in the case of (9). Again, we assume that n^2 is piecewise constant with polygonal interfaces with a finite number of corners.

Theorem 3. *Let λ be an eigenvalue of* (11) *with multiplicity m and corresponding m-dimensional eigenspace E. Then for sufficiently large G and sufficiently small $\Delta > 0$ there exist m eigenvalues $\lambda_1, \ldots, \lambda_m$ of* (12) *(with n^2 replaced by $\widetilde{n}^2$) counted according to multiplicity and corresponding eigenspaces $E_1, \ldots, E_m$ such that for any $s > 0$ we have*

$$\begin{aligned}
\delta_{H_p^1}\left(E, \bigoplus_{j=1}^m E_j\right) &\lesssim_s \Delta^{3/2} + \Delta^{-s} G^{-3/2-s}, \quad and \\
|\lambda - \lambda_j| &\lesssim_s \Delta^{3/2} + \Delta^{-2s} G^{-3-2s}, \quad for \ j = 1, \ldots, m.
\end{aligned}$$

---

[3]The notation $C \lesssim D$ here and below means that C/D is bounded uniformly with respect to any parameters. If we write $C \lesssim_x D$, then the bound may depend on the parameter x.

The proof of this result, which is given in [14], is in two parts and relies on the same theory as above. First the error from regularisation is bounded using Strang's 2nd Lemma [5, Theorem 4.1.1] in a non-standard way. An important part of this step is to show that

$$\|n^2 - \widetilde{n}^2\|_{H_p^{-1}} \lesssim \Delta^{3/2}. \tag{15}$$

This is then used to show that the eigenfunction and eigenvalue error due to regularisation are $\mathcal{O}(\Delta^{3/2})$. Note that the error in the eigenvalue due to regularisation is not the square of the respective eigenfunction error. This fact is confirmed by the numerical experiments in [14] (see [14, Fig. 8.1]). However, the experiments also suggest that the eigenvalue error due to regularisation is $\mathcal{O}(\Delta^2)$, implying that Theorem 3 is not completely sharp for the eigenvalue error.

The planewave expansion error for the regularised problem uses the improved regularity, i.e. if u is an eigenfunction of (11) (with n^2 replaced by $\widetilde{n}^2$) then

$$\|u\|_{H_p^s} \lesssim_s C(\Delta)\|u\|_{H_p^1} \qquad \text{where} \quad C(\Delta) := \begin{cases} 1, & \text{if } s < \frac{5}{2}, \\ (1 + \log(\Delta^{-1}))^{1/2}, & \text{if } s = \frac{5}{2}, \\ \Delta^{-s+5/2}, & \text{if } s > \frac{5}{2}, \end{cases}$$

for any $s \in \mathbb{R}$. This leads to an eigenfunction error that is $\mathcal{O}(\Delta^{-s}G^{-3/2-s})$ and an eigenvalue error that is $\mathcal{O}(\Delta^{-2s}G^{-3-2s})$ for $s > 0$. Choosing s large improves these errors with respect to G but there is a penalty that depends on the size of the regularisation parameter. The final result in the theorem is obtained by using the triangle inequality.

As explained in [14], by taking $\Delta = \mathcal{O}(G^r)$, for some $r \in \mathbb{R}$, we can try to balance the two error terms to obtain the optimal choice of regularisation parameter. There is no choice for r that leads to a practical or observable improvement of the convergence with respect to that of the un-regularised, plain vanilla planewave expansion method for (9). The numerical simulations in [14] (see [14, Fig. 8.2]) confirm that regularisation never improves the accuracy of the planewave expansion method for (9). For other types of regularisation we expect similar results.

Although the convergence rates in the case of the un-simplified PCF eigenproblem (5) are lower (as mentioned already), the numerical experiments in Section 4.3 still lead to the same conclusions about regularisation. No choice of regularisation parameter appears to improve the accuracy of the planewave expansion method with respect to the un-regularised plain vanilla method.

5.2. Analysis of the sampling method

The main new theoretical result of this paper is to extend the analysis for (9) in [14] to the planewave expansion method with sampling, as described in Section 3.3. There are two error contributions: the error due to planewave expansion and the sampling error. The analysis is rather technical, so we provide a succession of lemmas that build towards the main result, Theorem 7. Lemmas 4 and 5 bound the sampling error, Lemma 6 combines the sampling error with the planewave expansion error, and finally Theorem 7 will apply the general theory of Babuska and Osborn [2] to obtain eigenvalue and eigenfunction error bounds. As in earlier sections we assume throughout that n^2 is piecewise constant with polygonal interfaces with a finite number of corners and that it is periodic on a square Bravais lattice.

We begin by defining the standard mollifier $J \in C^\infty(\mathbb{R}^2)$ by

$$J(\mathbf{x}) := C \exp\left(\frac{1}{|\mathbf{x}|^2 - 1}\right), \quad \text{for } |\mathbf{x}| < 1, \quad \text{and} \quad J(\mathbf{x}) := 0, \quad \text{for } |\mathbf{x}| \geq 1,$$

15

where C is a constant such that $\int_{\mathbb{R}^2} J(\mathbf{x})d\mathbf{x} = 1$. For $\delta > 0$ we define $J_\delta(\mathbf{x}) := \delta^{-2}J(\delta^{-1}\mathbf{x})$. Then for any $f \in L^1_{loc}(\mathbb{R}^2)$ we define $f^{(\delta)} \in C^\infty(\mathbb{R}^2)$ by $f^{(\delta)} := J_\delta * f$. The following result is an important technical lemma and can also be found in [13, Lemma 4.37].

Lemma 4. *Let f be piecewise constant with polygonal interfaces with a finite number of corners. Then for any $0 < \delta < 1/2$ and $\epsilon > 0$ we have*

$$\|f^{(\delta)}\|_{H_p^s} \lesssim_{s,\epsilon} \begin{cases} 1 & \text{if } s < \frac{1}{2}, \\ \delta^{-s+\frac{1}{2}-\epsilon} & \text{if } s \geq \frac{1}{2}, \end{cases} \quad \text{and} \quad \|f - f^{(\delta)}\|_{H_p^s} \lesssim_s \delta^{-s+\frac{1}{2}} \quad \text{if } -\frac{3}{2} < s < \frac{1}{2}.$$

Proof. It follows from the properties of convolution that $[f^{(\delta)}]_\mathbf{g} = [J_\delta]_\mathbf{g}[f]_\mathbf{g}$, for all $\mathbf{g} \in \mathbb{G}$. Moreover, from the definition of J_δ, it follows that

$$|[J_\delta]_\mathbf{g}| = \left| \int_\Omega J_\delta(\mathbf{x})e^{-i\mathbf{g}\cdot\mathbf{x}}d\mathbf{x} \right| \leq \int_\Omega J_\delta(\mathbf{x})d\mathbf{x} = 1, \quad \text{for all } \mathbf{g} \in \mathbb{G}.$$

Therefore, $|[f^{(\delta)}]_\mathbf{g}| = |[J_\delta]_\mathbf{g}[f]_\mathbf{g}| \leq |[f]_\mathbf{g}|$, and so $\|f^{(\delta)}\|_{H_p^s} \leq \|f\|_{H_p^s} \lesssim_s 1$ for $s < 1/2$.

For any $t \in \mathbb{N} \cup \{0\}$ and $0 \neq \mathbf{g} \in \mathbb{G}$, suppose (without loss of generality) that $|g_1| \geq |g_2|$. Then $|\mathbf{g}| \lesssim |g_1|$ and integration by parts gives us

$$|\mathbf{g}|^t|[J_\delta]_\mathbf{g}| = |\mathbf{g}|^t \left| \left(\frac{-1}{ig_1} \right)^t \int_\Omega (\partial_x^t J_\delta)(\mathbf{x})e^{-i\mathbf{g}\cdot\mathbf{x}}d\mathbf{x} \right| \lesssim \delta^{-2-t} \left| \int_{|\mathbf{x}|<\delta} (\partial_x^t J)(\delta^{-1}\mathbf{x})e^{-i\mathbf{g}\cdot\mathbf{x}}d\mathbf{x} \right| \lesssim_t \delta^{-t}.$$

For any $s \geq 1/2$ and $t \in \mathbb{N} \cup \{0\}$ with $t > s - 1/2$, it follows, using the definition of $\|\cdot\|_{H_p^s}$, that

$$\begin{aligned}
\|f^{(\delta)}\|_{H_p^s}^2 &= |[f^{(\delta)}]_\mathbf{o}|^2 + \sum_{0 \neq \mathbf{g} \in \mathbb{G}} |\mathbf{g}|^{2s}|[f^{(\delta)}]_\mathbf{g}|^2 \\
&\lesssim_t |[f]_\mathbf{o}|^2 + \delta^{-2t} \sum_{0 \neq \mathbf{g} \in \mathbb{G}} |\mathbf{g}|^{2s-2t}|[f]_\mathbf{g}|^2 \leq \delta^{-2t}\|f\|_{H_p^{s-t}}^2 \lesssim_{s,t} \delta^{-2t}.
\end{aligned}$$

Using interpolation between periodic Sobolev spaces we obtain the first result in Lemma 4:

$$\|f^{(\delta)}\|_{H_p^s} \lesssim_{s,\epsilon} \begin{cases} 1 & \text{if } s < \frac{1}{2}, \\ \delta^{-s+\frac{1}{2}-\epsilon} & \text{if } s \geq \frac{1}{2}. \end{cases}$$

To show that $\|f - f^{(\delta)}\|_{H_p^s} \lesssim_s \delta^{-s+1/2}$, for $-3/2 < s < 1/2$, note first that $[f - f^{(\delta)}]_\mathbf{o} = 0$ and

$$|[f - f^{(\delta)}]_\mathbf{g}| \leq |[f]_\mathbf{g}| + |[f^{(\delta)}]_\mathbf{g}| \leq 2|[f]_\mathbf{g}|, \quad \text{for all } \mathbf{g} \in \mathbb{G}. \tag{16}$$

Moreover, for any $\mathbf{g} \in \mathbb{G}$ with $|\mathbf{g}| \leq \delta^{-1}$, we have

$$\begin{aligned}
|[f - f^{(\delta)}]_\mathbf{g}| &= |[f]_\mathbf{g}| \left| \int_{|\mathbf{x}|\leq 1} J(\mathbf{x})(1 - e^{-i\delta\mathbf{g}\cdot\mathbf{x}})d\mathbf{x} \right| \\
&\leq 2|[f]_\mathbf{g}|\|J\|_\infty \int_{[-1,1]^2} (1 - \cos(\delta g_1 x)\cos(\delta g_2 y))d\mathbf{x} \\
&= 8|[f]_\mathbf{g}|\|J\|_\infty \left(1 - \frac{\sin(\delta g_1)}{\delta g_1}\frac{\sin(\delta g_2)}{\delta g_2} \right).
\end{aligned}$$

Now, using the fact that $\frac{\sin A}{A} \geq 1 - \frac{A^2}{6}$, for $A^2 \leq 42$, we get

$$|[f - f^{(\delta)}]_\mathbf{g}| \leq \frac{4}{3}|[f]_\mathbf{g}|\|J\|_\infty \delta^2|\mathbf{g}|^2 \lesssim \delta^2|\mathbf{g}|^2|[f]_\mathbf{g}|^2 \tag{17}$$

16

To complete the proof we require a result from [14, Prop. 3.5] which implies that for any piecewise constant f with polygonal interfaces and a finite number of corners,

$$\sum_{|g_1|+|g_2|=h} |[f]_{\mathbf{g}}|^2 \lesssim h^{-2}. \tag{18}$$

Thus, it follows from (16)–(18) that for any $-3/2 < s < 1/2$,

$$
\begin{aligned}
\|f - f^{(\delta)}\|_{H_p^s}^2 &\lesssim \delta^4 \sum_{1 \le |g_1|+|g_2| \le \delta^{-1}} |\mathbf{g}|^{2s+4} |[f]_{\mathbf{g}}|^2 + \sum_{|g_1|+|g_2| > \delta^{-1}} |\mathbf{g}|^{2s} |[f]_{\mathbf{g}}|^2 \\
&\lesssim \delta^4 \sum_{h=1}^{\lfloor \delta^{-1} \rfloor} h^{2s+2} + \sum_{h=\lceil \delta^{-1} \rceil}^{\infty} h^{2s-2} \lesssim_s \delta^{1-2s}.
\end{aligned}
$$ □

The following lemma is the sampling version of (15) and its proof relies on Lemma 4.

Lemma 5. $\|n^2 - Q_M n^2\|_{L_p^2} \lesssim_\epsilon M^{-1/2+\epsilon}$ *for all $\epsilon > 0$.*

Proof. For ease of notation set $f := n^2$. Ω may be divided into M^2 square subdomains $S(\mathbf{x}, \frac{1}{2M}) := \{\mathbf{y} \in \mathbb{R}^2 : |x_i - y_i| < \frac{1}{2M}, i = 1, 2\}$, for any $\mathbf{x} \in \mathbb{B}_M$. Recall (8) and define a periodic piecewise constant function f_M such that

$$f_M(\mathbf{y}) := Q_M f(\mathbf{x}) \qquad \forall \mathbf{y} \in S(\mathbf{x}, \tfrac{1}{2M}), \mathbf{x} \in \mathbb{B}_M.$$

Now for any $\delta \le (2M)^{-1}$, $Q_M f(\mathbf{x}) = f_M(\mathbf{x}) = f_M^{(\delta)}(\mathbf{x})$ for all $\mathbf{x} \in \mathbb{B}_M$, and so $Q_M f = Q_M f_M^{(\delta)}$. Moreover, for any $v \in H_p^t$ with $t > 1$, $\|v - Q_M v\|_{L_p^2} \lesssim_t M^{-t} \|v\|_{H_p^t}$ (cf. [19, Theorem 8.5.3]). Hence, we can deduce from Lemma 4 that for any $\epsilon > 0$

$$\|f_M - Q_M f\|_{L_p^2} \le \|f_M - f_M^{(\delta)}\|_{L_p^2} + \|f_M^{(\delta)} - Q_M f_M^{(\delta)}\|_{L_p^2} \lesssim_{t,\epsilon} \delta^{1/2} + M^{-t}\delta^{-t+1/2-\epsilon}. \tag{19}$$

To bound the error between f and f_M, let $f_{max} := \operatorname{esssup}_{\mathbf{x} \in \Omega} f(\mathbf{x})$ and $f_{min} := \operatorname{essinf}_{\mathbf{x} \in \Omega} f(\mathbf{x})$. Since f is piecewise constant with polygonal interfaces with finitely many corners, f and f_M differ only on $N_{\text{diff}} = \mathcal{O}(M)$ of the square subdomains $S(\mathbf{x}, \frac{1}{2M})$. Hence,

$$\|f - f_M\|_{L_p^2}^2 \le N_{\text{diff}}(f_{max} - f_{min})^2 M^{-2} \lesssim M^{-1}. \tag{20}$$

The final result follows from (19) and (20) via the triangle inequality for $\delta = (2M)^{-1}$. □

Recall that $T : L_p^2 \to H_p^1$ is the solution operator corresponding to (11) defined in (13), and define equivalently a solution operator $T_{M,G} : L_p^2 \to \mathcal{S}_G \subset H_p^1$ for the discrete eigenvalue problem with sampling. To be precise, for any $f \in L_p^2$ define $T_{M,G} f \in \mathcal{S}_G$ by

$$a_M(T_{M,G} f, v) = b(f, v), \qquad \text{for all } v \in \mathcal{S}_G,$$

where

$$a_M(u, v) := \int_\Omega (\nabla_t + i\boldsymbol{\xi}) u \cdot \overline{(\nabla_t + i\boldsymbol{\xi}) v} + (\sigma - k^2 Q_M n^2) u \overline{v} \, \mathrm{d}x \mathrm{d}y.$$

The following lemma combines the sampling error and the planewave expansion error to obtain the error between the solution operators $T_{M,G}$ and T. This type of result is essential for the general theory in [2] which we aim to apply below and which is stated in terms of solution operators.

Lemma 6. $\|T - T_{M,G}\|_{H_p^1 \to H_p^1} \lesssim_\epsilon G^{-3/2+\epsilon} + M^{-1/2+\epsilon}$,   *for any $\epsilon > 0$.*

Proof. Let P_G define the orthogonal projection onto $\mathcal{S}_G$ (i.e. $[P_G f]_{\mathbf{g}} = [f]_{\mathbf{g}}$ for all $\mathbf{g} \in \mathbb{G}_G$ and $[P_G f]_{\mathbf{g}} = 0$ otherwise). By standard arguments, for any $v \in H_p^{1+s}$ with $s > 0$, we have $\|v - P_G v\|_{H_p^1} \le G^{-s} \|v\|_{H_p^{1+s}}$ (c.f. [19, Lemma 8.5.1] or [13, Lemma 3.30]), and thus by Strang's 2nd Lemma (c.f. [5, Theorem 4.1.1]) and the fact that P_G is an orthogonal projection we get

$$
\begin{aligned}
\|Tf - T_{M,G}f\|_{H_p^1} &\lesssim \inf_{v \in \mathcal{S}_G} \left\{ \|Tf - v\|_{H_p^1} + \sup_{w \in \mathcal{S}_G} \frac{|a(v,w) - a_Q(v,w)|}{\|w\|_{H_p^1}} \right\} \\
&\le \|Tf - P_G Tf\|_{H_p^1} + \sup_{w \in \mathcal{S}_G} \frac{|a(P_G Tf, w) - a_Q(P_G Tf, w)|}{\|w\|_{H_p^1}} \\
&\le G^{-3/2+\epsilon} \|Tf\|_{H_p^{5/2-\epsilon}} + k^2 \|Tf\|_\infty \|n^2 - Q_M n^2\|_{H_p^{-1}}.
\end{aligned}
$$

Using Sobolev embedding for C^0 in $H_p^{5/2-\epsilon}$ and for H_p^{-1} in L_p^2 together with (14) this implies

$$
\|Tf - T_{M,G}f\|_{H_p^1} \lesssim (G^{-3/2+\epsilon} + \|n^2 - Q_M n^2\|_{L_p^2}) \|f\|_{H_p^1}
$$

and the result follows from Lemma 5. $\qquad\square$

The following theorem follows directly from Lemma 6 and the general theory in [2]. For a complete proof see [13].

Theorem 7. *Let λ be an eigenvalue of* (11) *with multiplicity m and corresponding m-dimensional eigenspace E. Then for sufficiently large G and M, and arbitrarily small $\epsilon > 0$ there exist m eigenvalues $\lambda_1, \ldots, \lambda_m$ of* (12) *(with n^2 replaced by $Q_M n^2$), counted according to multiplicity, as well as corresponding eigenspaces $E_1, \ldots, E_m$ such that*

$$
\begin{aligned}
\delta_{H_p^1} \left(E, \bigoplus_{j=1}^m E_j \right) &\lesssim_\epsilon G^{-3/2+\epsilon} + M^{-1/2+\epsilon}, \quad \text{and} \\
|\lambda - \lambda_j| &\lesssim_\epsilon G^{-3+\epsilon} + M^{-1/2+\epsilon}, \quad \text{for } j = 1, \ldots, m.
\end{aligned}
$$

However, even though we proved the convergence of the sampling method rigorously, the order of $1/2$ for the sampling error does not seem to be sharp. The numerical results in Figure 8 suggest that the sampling error in the eigenfunctions and in the eigenvalues is $\mathcal{O}(M^{-1})$ for problem (9). We suspect that the reason for this loss of half an order in our proof is due to the inequality $\|n^2 - Q_M n^2\|_{H_p^{-1}} \le \|n^2 - Q_M n^2\|_{L_p^2}$ we used in the proof of Lemma 6, which is probably not sharp.

To optimise the error we consider $M = \mathcal{O}(G^r)$ for different values of $r \in \mathbb{R}$. The observed convergence rate of $\mathcal{O}(M^{-1})$ for the sampling error in the eigenfunctions suggests that $r \ge 3/2$ is necessary to recover the $\mathcal{O}(G^{-3/2+\epsilon})$ convergence of the error in the eigenfunctions due to planewave expansion. To optimise the error in the eigenvalues we should take $r \ge 3$. The effect of choosing different r on the error is tested numerically in Figure 9. It seems to confirm that a certain amount of oversampling is necessary to recover the convergence rate of the plain vanilla version (which uses exact Fourier coefficients). Especially for the eigenvalues, the error due to sampling is relatively large and so M must be chosen significantly larger than G to avoid that the sampling error dominates. This means that at least asymptotically, for $r > 1$, the additional FFT necessary to sample n^2 which requires $\mathcal{O}(M^2 \log M) = \mathcal{O}(G^{2r} \log G)$ operations becomes the dominant part in terms of CPU time and memory requirements. However, since this additional FFT is computed only once at the start, this does not manifest itself in the CPU time for typical practical grid
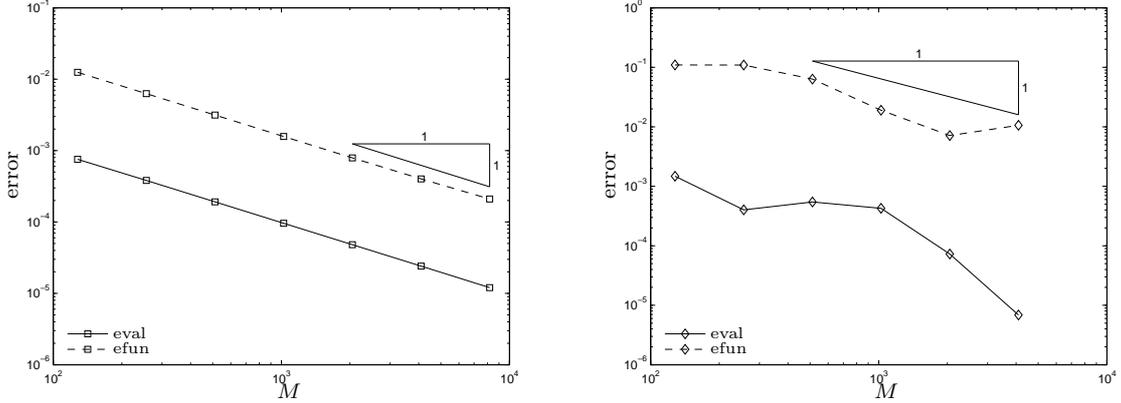
Figure 8: Planewave expansion method with sampling applied to (9) for Examples 1 (left) and 2 (right). Plotting the eigenfunction error in H_p^1 (`efun`) and the relative eigenvalue error (`eval`) for 1st eigenpair versus M (using $G = 2^8 - 1$, $\boldsymbol{\xi} = (\pi, \pi)$ in Example 1 and $\boldsymbol{\xi} = (\frac{\pi}{5}, \frac{\pi}{5})$ in Example 2).
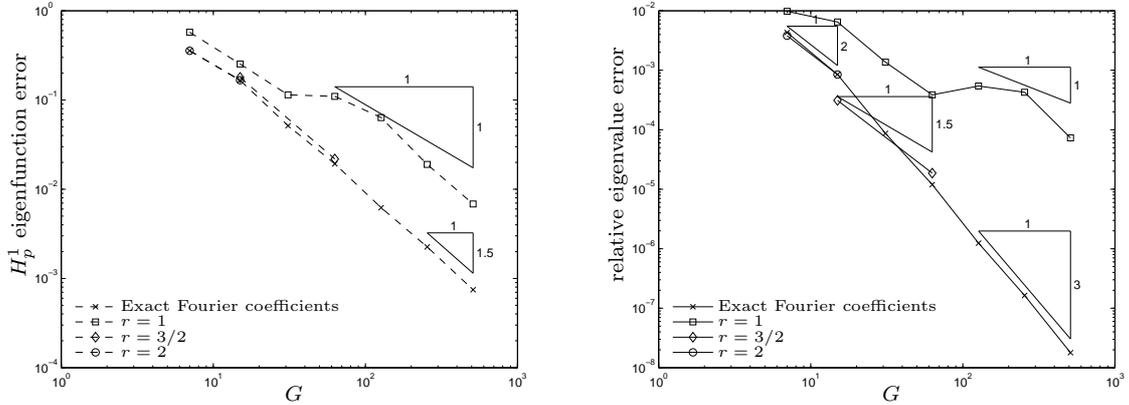
Figure 9: Planewave expansion method with sampling applied to (9) for Example 2. Plotting the eigenfunction error in H_p^1 (left) and the relative eigenvalue error (right) for 1st eigenpair versus G (using exact Fourier coefficients as well as $M = \mathcal{O}(G^r)$ for different choices of r; $\boldsymbol{\xi} = (\frac{\pi}{5}, \frac{\pi}{5})$).

sizes. However, the additional memory requirements are usually a real limitation on the amount of oversampling that can be employed and thus also on the overall convergence rate of the method. In our simulations $r = 2$ was the maximum amount of oversampling possible due to memory limitations.

5.3. Combining sampling and regularisation

To finish let us consider both modifications of the planewave expansion method together, i.e. regularization *and* sampling. For suitably chosen smoothing parameter $\Delta > 0$ and sampling parameter $M \in \mathbb{N}$, we replace n^2 with $n_{\Delta,M}^2 := \mathcal{G}_\Delta * (Q_M n^2)$.

In the case of the Schrödinger operator (9), the analysis of this combined method is simply a corollary of our previous results. Since $\exp(-|\mathbf{g}|^2 \Delta^2 / 2) \leq 1$ we have $\|\mathcal{G}_\Delta * v\|_{H_p^s} \leq \|v\|_{H_p^s}$ for any $s \in \mathbb{R}$, and so it follows from (15) and Lemma 5 that for any $\epsilon > 0$

$$\|n^2 - n_{\Delta,M}^2\|_{H_p^{-1}} \leq \|n^2 - \tilde{n}^2\|_{H_p^{-1}} + \|\mathcal{G}_\Delta * (n^2 - Q_M n^2)\|_{H_p^{-1}} \lesssim_\epsilon \Delta^{-1/2} + M^{-1/2+\epsilon}.$$

By proceeding as in the proof of Lemma 6 and Theorem 7 we obtain the following result.
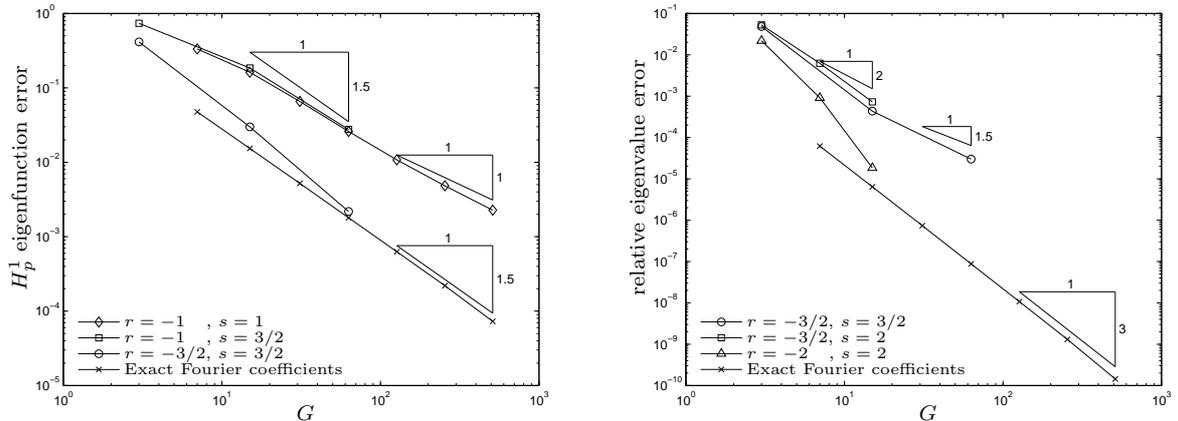
19

Figure 10: Planewave expansion method with regularisation *and* sampling applied to (9) for Example 1. Plotting the error for the 1st eigenpair versus G with exact Fourier coefficients and with $\Delta = G^r$ and $M = \mathcal{O}(G^s)$ for different choices of r and s (left: eigenfunction error; right: eigenvalue error; $\boldsymbol{\xi} = (0,0)$).

Theorem 8. *Let λ be an eigenvalue of (11) with multiplicity m and corresponding m-dimensional eigenspace E. Then for sufficiently large G and M, sufficiently small $\Delta > 0$, and arbitrarily small $\epsilon > 0$ there exist m eigenvalues of (12) (with n^2 replaced by $n_{\Delta,M}^2$), counted according to multiplicity, and corresponding eigenspaces $E_1, \ldots, E_m$ such that*

$$\delta_{H_p^1}\left(E, \bigoplus_{j=1}^m E_j\right) \lesssim_\epsilon G^{-3/2+\epsilon} + \Delta^{3/2} + M^{-1/2+\epsilon}, \quad and$$
$$|\lambda - \lambda_j| \lesssim_\epsilon G^{-3+\epsilon} + \Delta^{3/2} + M^{-1/2+\epsilon}, \quad for \ j = 1, \ldots, m.$$

In Figure 10 we report some numerical experiments for Example 1, using the planewave expansion method with regularisation and sampling for problem (9). We choose again $\Delta = G^r$ and $M = \mathcal{O}(G^s)$ for different values $r, s \in \mathbb{R}$. We know already from above that the rate for the sampling error is not sharp and that the rate for the smoothing error in the case of the eigenvalues is not sharp either. Hence using the numerically observed rates for those errors we expect

$$\delta_{H_p^1}\left(E, \bigoplus_{j=1}^m E_j\right) \lesssim G^{-3/2} + \Delta^{3/2} + M^{-1} \quad \text{and} \quad |\lambda - \lambda_j| \lesssim G^{-3} + \Delta^2 + M^{-1}.$$

Therefore to recover the convergence rates with exact Fourier coefficients (i.e. $\mathcal{O}(G^{-3/2})$ for eigenfunctions and $\mathcal{O}(G^{-3})$ for eigenvalues) it is sufficient to take $r = -1$ and $s = 3/2$ when considering the eigenvector error, and $r = -3/2$ and $s = 3$ when considering the eigenvalue error. However, the additional computational cost and memory requirements for sampling restrict us to $s \le 2$ and our observations in Figure 10 suggest that the best choice is to take $s = 3/2$ for eigenfunctions and $s = 2$ (largest practically possible) for eigenvalues, with little or no regularisation.

6. Conclusions

Photonic crystal fibres are a novel generation of optical devices with many potential applications. Simulating the propagation of light in PCFs is thus of great interest. Through rigorous analysis of simplified model problems and through numerical experimentation on the original PCF model problem we explored in this paper the potential and the limitations of planewave expansion methods for PCF problems. Due to the discontinuous refractive index in PCFs, exponential

convergence of the planewave expansion method can clearly not be expected and indeed the convergence rate is in all cases limited by the regularity of the eigenfunctions that are approximated. Especially in the case of the un-simplified full PCF model problem this limits the convergence rate significantly. Regularisation of the coefficient functions does not mitigate this effect and the numerical experiments in this paper clearly confirm this.

In practice, it is usually necessary to approximate the Fourier coefficients of the coefficient functions via sampling techniques. This leads to an additional error. We showed numerically that this error is usually dominating (especially in the eigenvalue error for a simplified Schrödinger–type problem) unless the sampling is carried out on a significantly finer FFT grid than the planewave expansion. Extending the theory in [14], we managed to also rigorously prove the convergence of the sampling method for a simplified Schrödinger–type model problem.

Acknowledgements

References

[1] N. Ashcroft, N. Mermin, Solid State Physics, Saunders College, Philadelphia, 1976.

[2] I. Babuska, J. Osborn, Eigenvalue problems, in: Finite Element Methods (Part 1), volume 2 of *Handbook of Numerical Analysis*, Elsevier, 1991, pp. 641–787.

[3] T. Birks, D. Bird, T. Hedley, J. Pottage, P. Russell, Scaling laws and vector effects in bandgap-guiding fibres, Optics Express 12 (2004) 69–74.

[4] Y. Cao, Z. Hou, Y. Liu, Convergence problem of plane-wave expansion method for phononic crystals, Physics Letters A 327 (2004) 247–253.

[5] P.G. Ciarlet, The Finite Element Method for Elliptic Problems, SIAM, Philadelphia, 2002.

[6] J. Joannopoulos, S. Johnson, J. Winn, R. Meade, Photonic Crystals Molding the Flow of Light, Princeton University Press, Princeton, second edition, 2008.

[7] S. Johnson, J. Joannopoulos, Block-iterative frequency-domain methods for Maxwell's equations in a planewave basis, Optics Express 8 (2001) 173–190.

[8] C. Kelley, Iterative methods for linear and nonlinear equations, volume 16 of *Frontiers in applied mathematics*, SIAM, Philadelphia, 1995.

[9] P. Kuchment, The mathematical theory of photonic crystals, in: G. Bao, L. Cowsar, W. Masters (Eds.), Mathematical Modelling in Optical Science, Frontiers in Applied Mathematics, SIAM, 2001, pp. 207–272.

[10] R. Lehoucq, D. Sorensen, C.Yang, ARPACK users' guide, SIAM, Philadelphia, 1998.

[11] R. Meade, A. Rappe, K. Brommer, J. Joannopoulos, O. Alerhand, Accurate theoretical analysis of photonic band-gap materials, Physical Review B 48 (1993) 8434–8437.

[12] M. Min, D. Gottlieb, On the convergence of the fourier approximation for eigenvalues and eigenfunctions of discontinuous problems, SIAM J. Numer. Anal. 40 (2003) 2254–2269.

[13] R. Norton, Numerical Computation of Band Gaps in Photonic Crystal Fibres, Ph.D. thesis, University of Bath, England, 2008.

[14] R. Norton, R. Scheichl, Convergence analysis of planewave expansion methods for 2d Schrödinger operators with discontinuous periodic potentials, SIAM J. Numer. Anal. 47 (2010) 4356–4380.

[15] G. Pearce, Plane-wave methods for modelling photonic crystal fibre, Ph.D. thesis, University of Bath, England, 2006.

[16] G. Pearce, T. Hedley, D. Bird, Adaptive curvilinear coordinates in a plane-wave solution of Maxwell's equations in photonic crystals, Physical Review B 71 (2005).

[17] G. Pearce, J. Pottage, D. Bird, P. Roberts, J. Knight, P. Russell, Hollow-core pcf for guidance in the mid to far infra-red, Optics Express 13 (2005) 6937–6945.

[18] J. Pottage, D. Bird, T. Hedley, T. Birks, J. Knight, P. Russell, Robust photonic band gaps for hollow core guidance in pcf made from high index glass, Optics Express 11 (2003) 2854–2861.

[19] J. Saranen, G. Vainikko, Periodic integral and pseudodifferential equations with numerical approximation, Springer, 2000.

[20] S. Soussi, Convergence of the supercell method for defect modes calculations in photonic crystals, SIAM J. Numer. Anal. 43 (2005) 1175–1201.

[21] H. Sozuer, J. Haus, Photonic bands: Convergence problems with the planewave method, Physical Review B 45 (1992) 13962–13973.